The influence of the relative position of the thiophene and pyrrole rings in donor–acceptor thienylpyrrolyl-benzothiazole derivatives. A photophysical and theoretical investigation

João Pina,*[a] J. Sérgio Seixas de Melo,*[a] Rosa M. F. Batista,[b] Susana P. G. Costa[b] and M. Manuela M. Raposo*[b]

Received 4th February 2010, Accepted 12th April 2010
DOI: 10.1039/c002434a

A detailed spectroscopic and photophysical study has been carried out on a series of heterocyclic compounds—known to display nonlinear optical properties—consisting on a electron donating thienylpyrrolyl π-conjugated system functionalized with an electron acceptor benzothiazole moiety. The absorption, emission and triplet–triplet absorption together with all relevant quantum yields (fluorescence, intersystem crossing and internal conversion), excited state lifetimes and the overall set of deactivation rate constants (k_F, k_{IC} and k_{ISC}) were obtained in solution at room (293 K) and low (77 K) temperature. The optimized ground-state molecular geometries for the compounds together with the prediction of the lowest vertical one-electron excitation energy and the relevant molecular orbital contours for the compounds were also determined using density functional theory (DFT) at the B3LYP/3-21G* level. The experimental results showed that the photophysical properties are influenced by the relative position of the pyrrole and thiophene relative to the benzothiazole group.

Introduction

The research for nonlinear optical (NLO) materials has been the focus of intense research in due part to their potential in applications including optical data transmission and information processing.[1–5] High NLO responses are obtained when the materials possess large molecular hyperpolarizabilities and low optical loss.[6,7] A general approach to obtain materials with NLO properties consists of the synthesis of chromophores involving electron-donor and electron-acceptor groups linked through a π-conjugated spacer. The use of organic π-conjugated systems is particularly relevant in the development of NLO materials since, amongst other properties, they can show large nonlinearities, and display ultra-fast responses, because the electronic polarization is nearly instantaneous.[1] For these systems, optimization of the electron-donor and electron-acceptor characteristics of the substituents is needed to obtain maximum nonlinearity at a molecular level. For the π-conjugating bridge systems, several linear polyenes to various aromatic (heterocyclic) substituents have been used.[8–11] Included in these, easily delocalized five-membered rings (such as furan and thiophene based π-conjugated spacers) have proved to increase the hyperpolarizabilities of NLO chromophores.[1,6,7,12,13] This is in part due to the high chemical and thermal stability together with the displayed good optical properties which allow efficient π-electron delocalization.[12–15] Although less investigated, pyrrole containing chromophores as the conjugated bridge, were found to display enhanced NLO properties in comparison with their analogues with furan or thiophene.[16] This was attributed to the higher electron density in the pyrrole moiety compared to thiophene and furan which led to enhanced NLO effects.[17,18] This higher electron density (in the pyrrole ring) can be explained by the different electric dipole moment of pyrrole compared to thiophene and furan, with its direction from the heteroatom to the five-membered ring, thus enhancing the contribution of the n electrons of the nitrogen atom to the π-system. However, although the results showed that pyrrole moieties are promising building blocks for chromophores with enhanced NLO properties it was concluded that the increase or decrease of the molecular nonlinear activity on heteroaromatic systems depends on the nature of the aromatic rings as well as on the location of these heteroaromatic rings in the system.[19–22]

An additional advantage of the use of π-excessive heteroaromatic groups in the conjugated bridge is that they also act as donor groups.

Having in mind our recent work, concerning the synthesis and photophysical properties of benzothiazole derivatives in conjunction with five-membered heterocycles (thiophene and pyrrole)[21,23,24] we decided to investigate the effect of the presence and position of electron-rich and electron-deficient heterocycles on the photophysics of these compounds. The present work follows a previous report of the synthesis, the second-order hyperpolarizability (β) and thermal stability of 1-(alkyl)aryl-2-(2′-thienyl)pyrroles (acting as π–electron donors) end-terminated with a benzothiazole heterocycle (electron-withdrawing group).[21] We have previously found that the position of the electron-deficient benzothiazole on the thienyl-pyrrolyl system had a marked influence on the NLO properties. With the present paper, we extend this study to

[a] *Department of Chemistry, University of Coimbra, Rua Larga, 3004-535 Coimbra, Portugal. E-mail: jpina@qui.uc.pt, sseixas@ci.uc.pt*
[b] *Centro de Química, Universidade do Minho, Campus de Gualtar, 4710-057 Braga, Portugal. E-mail: mfox@quimica@uminho.pt*

the detailed spectroscopic (singlet and triplet state) and the photophysical properties in solution (at room and low temperature), together with the theoretical investigation (DFT) of the ground- and singlet excited state optimized geometries of these compounds.

Experimental

The thienylpyrrolyl-benzothiazoles **1a** and **2a–c** were synthesized as elsewhere described.[21] The solvents were all of spectroscopic or equivalent grade and used without further treatment. Absorption spectra and fluorescence were recorded on a Shimadzu UV-2100 and Horiba–Jobin–Ivon Fluorog 3–22 spectrometers respectively. Phosphorescence measurements were made in methylcyclohexane (MCH) glasses at 77 K and used a Horiba–Jobin–Ivon Fluorog 3–22 spectrometer equipped with a 1934D phosphorimeter unit and a 150 W pulsed xenon lamp. All the fluorescence and phosphorescence spectra were corrected for the wavelength response of the system.

The fluorescence quantum yields were measured using as standards terthiophene ($\phi_F = 0.057$) and quaterthiophene ($\phi_F = 0.18$) in MCH.[25] The fluorescence quantum yields at 77 K were obtained by comparison with the spectrum at 293 K run under identical experimental conditions and the ϕ_F value was obtained by assuming that $V_{77\ K}/V_{293\ K} = 0.8$.[26] Phosphorescence quantum yields were obtained using benzophenone in ethanol solution ($\phi_{Ph} = 0.84$) as standard.[26]

The molar extinction coefficients (ε) were obtained from the slope of the plot of the absorption with six solutions of different concentrations *vs.* the concentration (correlation values ≥ 0.999).

Fluorescence decays were measured using a home-built picosecond time correlated single photon counting (TCSPC) apparatus described elsewhere.[27] Fluorescence decays and the instrumental response function (IRF) where collected using 4096 channels, until 5×10^3 counts at maximum were reached. The full width at half maximum (FWHW) of the IRF was about 22 ps and was highly reproducible with identical system parameters. Deconvolution of the fluorescence decays curves was performed using the modulating functions previously reported.[28]

The experimental setup used to obtain triplet spectra and triplet yields has been described elsewhere.[29,30] First-order kinetics was observed for the decay of the lowest triplet state. Special care was taken in determining triplet yields, namely to have optically matched dilute solutions (abs ≈ 0.2 in a 10 mm square cell) and low laser energy (≤ 2 mJ) to avoid multiphoton and T–T annihilation effects.

The triplet molar absorption coefficients were obtained by the energy transfer method.[31] The triplet state molar absorption coefficients were determined using naphthalene, $\varepsilon_T = 24\,500\ M^{-1}\ cm^{-1}$ (415 nm) as triplet energy donor.[26] The concentrations for the thienylpyrrole-benzothiazoles were 10^{-5} M and they were dissolved in 1 mM methylcyclohexane solution of naphthalene. Before experiments, all solutions were degassed with nitrogen for 30 min and sealed.

The ϕ_T values were obtained by comparing the ΔO.D. at 525 nm of a benzene solution of benzophenone (bzph, the standard) and of the compound (cp, optically matched at the laser wavelength) using the equation:[32]

$$\phi_T^{cp} = \frac{\varepsilon_{TT}^{bzph}}{\varepsilon_{TT}^{cp}} \frac{\Delta OD_{max}^{cp}}{\Delta OD_{max}^{bzph}} \phi_T^{bzph} \quad (1)$$

Room-temperature singlet oxygen phosphorescence was detected in a Horiba–Jobin–Ivon SPEX Fluorog 3–22 equipped with a Hamamatsu R5509-42 photomultiplier cooled to 193 K in a liquid nitrogen chamber (Products for Research model PC176TSCE-005) The use of a Schott RG1000 filter was essential to eliminate from the infrared signal all of the first harmonic contribution of the sensitizer emission in the region below 850 nm. The sensitized phosphorescence emission spectra of singlet oxygen from optically matched solutions of the samples and that of reference were obtained in identical experimental conditions. The singlet oxygen formation quantum yield was then determined by comparing the integrated area under the sensitized emission spectra of singlet oxygen of the samples solutions ($\int I(\lambda)^{cp}\, d\lambda$) and that of the reference solution ($\int I(\lambda)^{ref}\, d\lambda$) and applying equation (2).

$$\phi_\Delta^{cp} = \frac{\int I(\lambda)^{cp}\, d\lambda}{\int I(\lambda)^{ref}\, d\lambda} \phi_\Delta^{ref} \quad (2)$$

with ϕ_Δ^{ref} the singlet oxygen formation quantum yield of the reference compound. 1*H*-Phenalen-1-one in toluene ($\phi_\Delta = 0.93$) was used as standard.[33]

The ground state molecular geometry was optimized using density functional theory (DFT) by means of the Gaussian 03 program,[34] under B3LYP/3-21G* level.[35,36] Optimal geometries were determined on isolated entities in a vacuum and no conformation restrictions were imposed. For the resulting optimized geometries time dependent DFT calculations (using the same functional and basis set as those in the previous calculations) were performed to predict the vertical electronic excitation energies. The excited-state geometries were optimized using the Hartree–Fock based single-excitation restricted configuration interaction (RCIS)[37] method with the 3-21G* basis set. Molecular orbital contours were plotted using Molekel 5.3.[38]

Results

Important features that will be considered in this study are the changes in the spectroscopic and photophysical properties induced by (i) the position of the benzothiazole moiety (linked to position 2 of the pyrrole or the thiophene ring) and (ii) the substitution on the nitrogen atom of the pyrrole ring. The structures of the investigated compounds are depicted in Scheme 1.

Singlet state

Fig. 1 presents the absorption and fluorescence emission spectra of the investigated thienylpyrrolyl-benzothiazole **1–2** derivatives in methylcyclohexane (MCH) solution at room and low temperature. These display absorption bands and wavelength maxima (Table 1) which are similar to those reported for the thienyl-benzothiazole derivatives, particularly when the

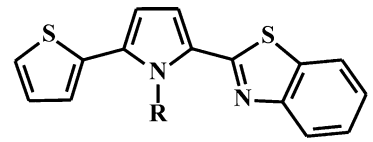

1a R= n-Pr

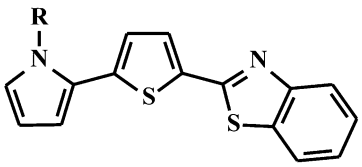

2a,b,c

a R= n-Pr
b R= 4-MeOPh
c R= 2,4-diMeOPh

Scheme 1

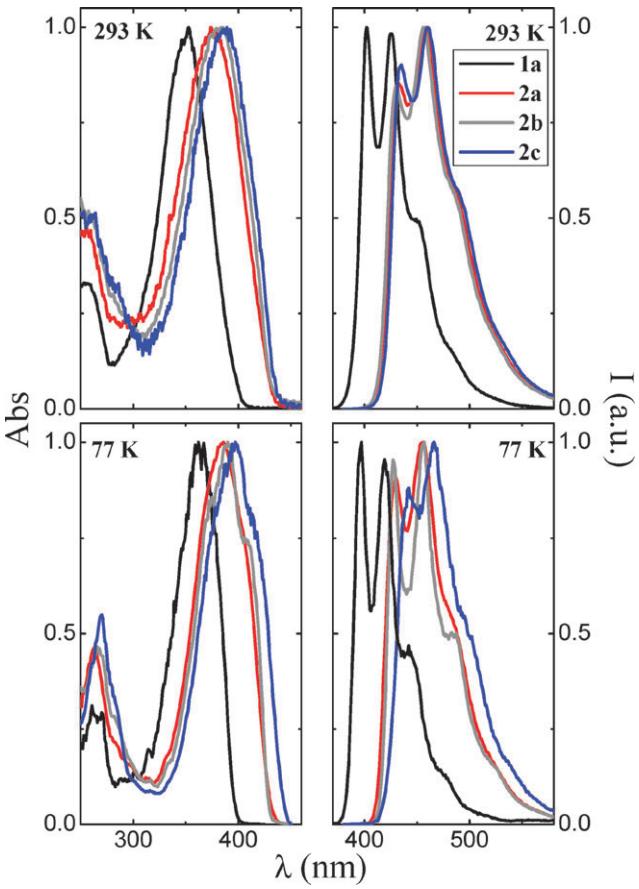

Fig. 1 Normalized absorption and fluorescence emission spectra for the thienylpyrrolyl-benzothiazoles **1–2** in methylcyclohexane solution at 293 and 77 K.

comparison is made between **2a** (and derivatives **2b** and **2c**) and the benzothiazole-bithienyl derivative (**BZT2a**),[39] showing that in terms of spectral characteristics the substitution of a thiophene with a pyrrole ring has no significant changes in the properties displayed by these compounds.

In order to get more insight on the electronic properties of the compounds the ground state geometry of these were optimized at the DFT/B3LYP/3.21G* level (Fig. 2). In addition, for **2a**, the singlet excited state geometry was optimized using the RCIS/3.21G* method and basis set (Fig. 3).

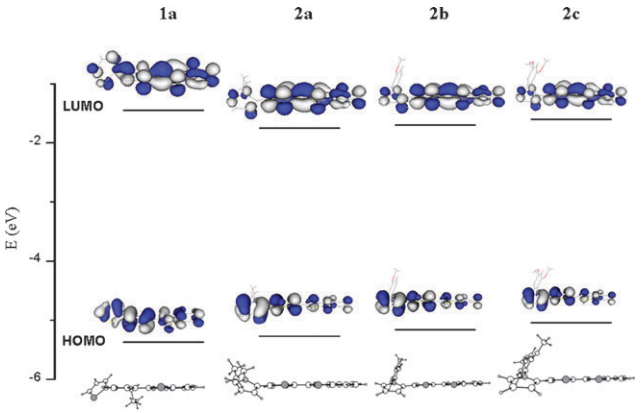

Fig. 2 B3LYP/3-21G* DFT optimized ground-state molecular structures for the thienylpyrrolyl-benzothiazoles **1–2** together with the relevant molecular orbital contours around the band gap.

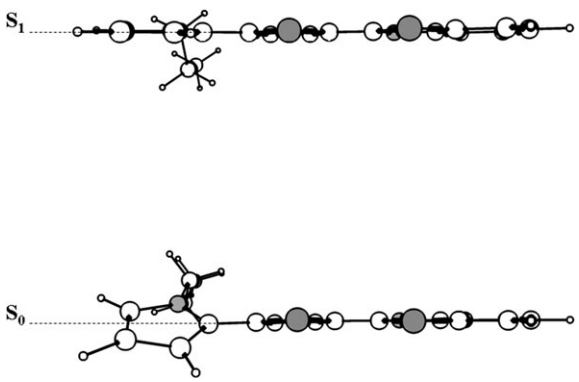

Fig. 3 DFT//B3LYP/3-21G* optimized lowest lying singlet (S_0) and the HF//RCIS/3-21G* singlet excited state (S_1) geometries for compound **2a**.

Fluorescence decays (collected at the emission wavelength maximum) were measured in solution at room temperature and were all seen to fit to monoexponential decay laws (see Fig. 4).

Triplet state

The triplet states of the oligomers were characterized from the transient triplet–triplet absorption spectra in toluene solution at 293 K (Fig. 5). In addition to ground state depletion at shorter wavelengths, the spectra show a broad and intense triplet absorption in the 410–700 nm region (see Fig. 5A).

For the thienylpyrrolyl-benzothiazoles phosphorescence was also investigated in methylcyclohexane glasses at 77 K and with our available current experimental setup we were only able to detect phosphorescence for compound **1a**. In this case a structured emission band with a shoulder at 575 nm and maximum at 610 nm was observed (see Fig. 5B). Compound **1a** presents a low phosphorescence quantum yield (ϕ_{Ph} = 0.005) in agreement to what was previously found for short thiophene oligomers,[25,29,40,41] thienyl-pyrrole oligomers[42] and oligothienyl-imidazole[43] derivatives. The phosphorescence lifetime (τ_{Ph}) for this compound was found to be 15 ms, see inset in Fig. 5B.

Table 1 Spectroscopic properties for the thienylpyrrolyl-benzothiazoles in toluene and methylcyclohexane (MCH) at 293 and 77 K

Compound	Solvent	$\lambda_{max}^{S_1 \leftarrow S_0}$/ nm (293 K)	$\lambda_{max}^{S_1 \leftarrow S_0}$/ nm (DFT)	$\lambda_{max}^{S_1 \leftarrow S_0}$/ nm (77 K)	$\lambda_{max}^{S_1 \leftarrow S_0}$/ nm (293 K)[a]	$\lambda_{max}^{S_1 \leftarrow S_0}$/ nm (77 K)[a]	$\lambda_{max}^{T_1 \rightarrow T_n}$/ nm (293 K)	ε_{SS}[b]/ M^{-1} cm^{-1}	ε_{TT}[b]/ M^{-1} cm^{-1}	Δ_{SS}[c]/cm^{-1} (293 K)
1a	Toluene	355	341		*410*, 432		560	28 600		3779
	MCH	353		362	*402*, 425, 450	*397*, 419, 442			9600	3453
2a	Toluene	380	381		455, *473*		480	18 100		5174
	MCH	375		385	432, *458*	430, *455*			6500	4833
2b	Toluene	386	385		450, *470*		475	12 100		4630
	MCH	380		390	429, *455*	427, *456*, 485			8850	4338
2c	Toluene	392	388		452, *473*		480	23 700		4369
	MCH	387		397	435, *460*	442, 465			8200	4101

[a] The italicized figures are the wavelength maxima. [b] Singlet (ε_{SS}) and triplet (ε_{TT}) molar extinction coefficients. [c] Stokes shift.

Singlet oxygen quantum yields were also obtained by comparing the sensitized emission spectra from singlet oxygen, obtained in optically matched solutions of the samples and that of the reference 1*H*-phenalen-1-one, Table 2 (for more details see experimental section).

Discussion

Spectroscopic behaviour

The absorption spectra of the thienylpyrrolyl benzothiazoles are broad and devoid of vibrational structure. This behavior is consistent with the fact that the degree of rotational freedom around the thiophene-pyrrole, thiophene-benzothiazole and pyrrole-benzothiazole allows the existence of an ensemble of conformers in the ground state leading to a broad (overlap of these multiple conformers) absorption. The placement of the benzothiazole moiety on the thiophene heterocycle on the thienylpyrrolyl system (**2a**), when compared to the derivative bearing the benzothiazole unit at the pyrrole ring (**1a**), leads to a red-shift in the absorption maxima in solution at 293 K by ≈25 nm (Table 1). This behaviour can be explained by a more extensive electron delocalization (increased intramolecular electron-transfer from the donor to the electron-acceptor group) with **2a**[21] which in turn leads to an increase in hyperpolarizability when going from **1a** (64×10^{-30} esu) to **2a** ($\approx 890 \times 10^{-30}$ esu). This is a well-known property of materials showing NLO properties[44] and was previously reported for benzothiazole-,[21] benzimidazole-[22] and dicyanovinyl-[20] substituted thienylpyrrole derivatives where it was observed that the increase in the hyperpolarizability values is accompanied by an increase in the absorption wavelength maxima. This observation is in agreement with previous studies where it was concluded that the increase (or decrease) of the molecular NLO activity on heteroaromatic systems is related to the nature of the aromatic rings and on the location of these heteroaromatic chromophores in the systems.[19–22,45] In our particular case the decrease in hyperpolarizability, when the benzothiazole unit is connected to the pyrrole (**1a**), indicates that the pyrrole unit is a less efficient π-conjugated bridge when compared to thiophene. This is due to the fact that the pyrrole unit is the most electron-rich five-membered heteroaromatic ring (thus displaying higher aromaticity than thiophene) and can counteract the electron-withdrawing effect of the benzothiazole unit, hindering the electron delocalization.[20–22,45]

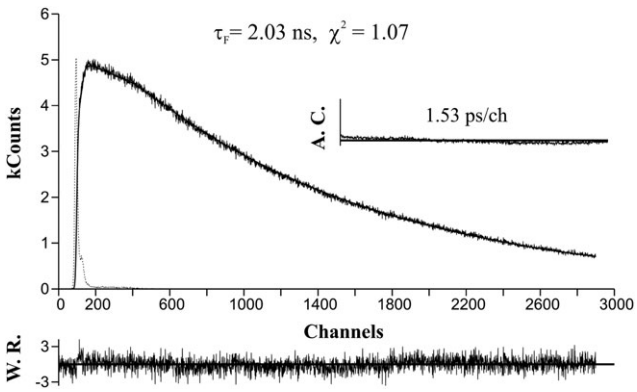

Fig. 4 Fluorescence decay for compound **2a** in toluene at 293 K obtained with λ_{exc} = 425 nm and collected at λ_{em} = 460 nm. For a better judgment of the quality of the fit, autocorrelation function (A.C.), weighted residuals (W.R.) and the chi-square value (χ^2) are also presented as insets. The dashed line in the decay is the pulse instrumental response.

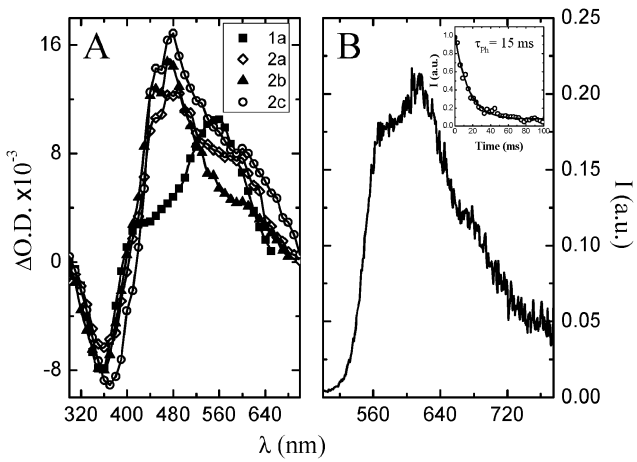

Fig. 5 (A) Transient triplet–triplet absorption spectra for the thienylpyrrolyl-benzothiazoles in toluene at 293 K. (B) Phosphorescence emission spectra for compound **1a** in MCH solution at 77 K. The phosphorescence emission decay is also presented in the inset.

For compounds **2a–c** replacement of alkyl for aryl substituents in the pyrrole moiety induces a slight red-shift (≈12 nm) in the absorption wavelength maxima.

Contrary to the absorption spectra, the fluorescence emission spectra display vibrational structure thus showing

Table 2 Photophysical properties including quantum yields (fluorescence, ϕ_F, internal conversion, ϕ_{IC}, triplet formation, ϕ_T, and sensitized singlet oxygen formation, ϕ_Δ), lifetimes (τ_F, τ_T), rate constants (k_F, k_{NR}, k_{IC}, k_{ISC}) for the thienylpyrrolyl-benzothiazoles in toluene and methylcyclohexane at 293 and 77 K[a]

Compound	Solvent	ϕ_F (293 K)	τ_F/ns (293 K)	ϕ_F (77 K)	ϕ_{IC} (293 K)	ϕ_T	ϕ_Δ	τ_T/s	k_F/ns^{-1} (293 K)	k_{NR}/ns^{-1} (293 K)	k_{IC}/ns^{-1} (293 K)	k_{ISC}/ns^{-1} (293 K)
1a	Toluene	0.17	0.540		0.20	0.63	0.61	7.75	0.315	1.54	0.380	1.17
	MCH	0.21		0.18								
2a	Toluene	0.70	2.03		0.12	0.18	0.11	6.06	0.345	0.148	0.059	0.089
	MCH	0.69		0.43								
2b	Toluene	0.73	2.01		0.16	0.11	0.11	25.0	0.363	0.134	0.080	0.055
	MCH	0.66		0.42								
2c	Toluene	0.69	2.00		0.19	0.12	0.10	16.5	0.345	0.155	0.095	0.060
	MCH	0.67		0.44								

[a] $k_F = \phi_F/\tau_F$; $k_{NR} = (1 - \phi_F)/\tau_F$; $k_{IC} = (1 - \phi_F - \phi_T)/\tau_F$; $k_{ISC} = \phi_T/\tau_F$; $\phi_{IC} = 1 - \phi_F - \phi_T$.

that different geometries are adopted in the ground- and singlet excited-state. In agreement with this behavior are the large Stokes-shift values (Δ_{SS}, Table 1) found for the compounds under study. More detail from the ground and excited states can be obtained from the analysis of the DFT calculations. From the ground-state optimized geometries (DFT calculations) it was seen that for compound **1a** a planar conformation is adopted by the pyrrolyl-benzothiazole moieties and the terminal thienyl unit presents a dihedral angle of $\approx 50^\circ$ with respect to the planar backbone (Fig. 2). For compounds **2a–c** a similar planar structure was found for the thienyl-benzothiazole chromophores and again the end-terminal unit (pyrrolyl) is slightly twisted, displaying a dihedral angle of $\approx 35^\circ$, **2a**, and $\approx 25^\circ$ for compounds **2c** and **2d** (Fig. 2). The shorter conjugation length found for **1a** can be explained by the more twisted (higher dihedral angle) end terminal thienyl group that acts as a conjugation barrier when compared to compounds **2a–c**.

From the TDDFT calculations on the previously optimized ground-state geometries it was possible to predict the lowest vertical one-electron excitation energy (Table 1). The predicted values 341 nm, **1a**, 381 nm, **2a**, 385 nm, **2b**, and 388 nm, **2c**, are in good agreement with the experimental values in solution (Table 1) which gives support for the calculated molecular geometries. Also worth noting is the fact that the calculated wavelength maxima, and consequently the decrease in the HOMO–LUMO energy difference, upon going from **1a** to **2a** accounts for the spectral red-shift observed in the absorption wavelength maxima (see Fig. 1 and 2).

The excited-state geometry was optimized for **2a** and it was seen that a total planarization of the compound backbone was achieved (Fig. 3). This, together with the analysis of the relevant molecular orbital contours (Fig. 2), where it was seen that going from the HOMO to the LUMO of the compounds a marked increase in the electron density cloud around the C–C bonds connecting the thienyl, pyrrolyl and benzothiazole moieties is observed, shows that a quinoidal-type structure should be adopted in the excited state. TDDFT calculation were performed on the previously optimized excited-state geometry allowing the determination of the vertical radiative transition between the excited- (S_1) and ground-state (S_0). The theoretical value (423 nm) found is in good agreement with the experimental fluorescence wavelength maxima found for this compound (see Table 1) thus giving, once again, support for the calculated geometry.

Upon going to low temperature a slight increase in vibrational resolution was seen in the absorption and emission spectra. Contrary to what is observed in absorption where $a \approx 10$ nm red-shift was observed when going from 293 to 77 K for the emission band no significant changes were found (see Table 1 and Fig. 1) thus indicating that similar geometries are adopted (quinoidal-like) in the excited state at 293 and 77 K. Similar behavior was reported previously for mixed furan-pyrrole-thiophene containing oligomers[42] and was attributed to a decrease of the relative population of more twisted conformers in the ground-state when going from 293 to 77 K. In this situation the ground- and excited-state potential energy curves become more vertically aligned such that the vertical transition is more probable to a lower vibrational level, thus resulting in the observed red-shift of the absorption wavelength maxima at 77 K.

Photophysical behaviour

The photophysical parameters obtained in solution at 293 and 77 K are shown in Table 2. From the overall data it can be seen that for all the compounds, with the exception of **1a** the radiative decay channel is the main excited-state deactivation channel. For compound **1a**, where the benzothiazole moiety is linked to the pyrrolyl unit, a decrease in the fluorescence quantum yield (ϕ_F) at 293 K when compared to compounds **2a–c**, was observed. In this case, the radiationless processes are dominant and from these, the intersystem crossing (which can be seen from the ϕ_T, and k_{ISC} parameters in Table 2) is the preferred pathway for the excited-state decay. It is interesting to note that both the photophysical and spectroscopic properties of compound **1a** are similar to the analogue thienyl-pyrrolyl-thienyl (SNS) oligomer.[42] A potential explanation for the observed behavior is that the less efficient delocalization of π-electrons seen for **1a** (influenced by the position of the pyrrole ring) induces a similar conjugation segment to that of SNS, and as a consequence, **1a** retains the characteristic photophysical properties of SNS. On the contrary, for **2a–c** because of the higher charge-transfer character in the compounds there is more involvement of the benzothiazole unit, thus enhancing the fluorescence

excited-state deactivation channel. The comparison between the bithienyl-benzothiazole (**BzT2a**)[39] and **2a** shows that the substitution of a thiophene by a pyrrole ring increases the deactivation through the radiative rate channel. Indeed for **BzT2a** the quantum yields are $\phi_F = 0.31$, $\phi_T = 0.52$ and $\phi_{IC} = 0.17$,[39] whereas with **2a** (Table 2) $\phi_F = 0.7$, $\phi_T = 0.18$ and $\phi_{IC} = 0.12$, respectively, thus showing that, going from **BZT2a** to **2a** the increase in fluorescence occurs with the concomitant decrease of the intersystem crossing process. For **1a** the low phosphorescence quantum yield and the high intersystem-crossing value indicate that the radiationless channel is the main route for the triplet state decay. In this case, from the onset of the phosphorescence emission band it was possible to estimate the triplet energy of **1a** (2.30 eV). From this and the singlet energy (3.18 eV, taken from the intersection between the normalized absorption and emission spectra) the singlet–triplet energy splitting, $\Delta E_{S_1-T_1} = 0.88$ eV, was obtained. The triplet energy value obtained is similar to the value found for the SNS oligomer (2.25 eV).[42]

Upon cooling to 77 K a decrease in the ϕ_F values was seen (again the exception was **1a**). A similar decrease in ϕ_F when going from 293 to 77 K was previously reported for the thienyl-benzothiazole[39] derivatives but contrast with the behavior of thiophene[25] and mixed furan-pyrrole-thiophene[42] oligomers where an increase or constancy of this value is generally observed. An explanation for the observed behavior resides, as previously discussed, in the fact that at 77 K the emission results from an excited-state with the same geometry and energy that at 293 K but to a more planar ground-state (with higher energy at 77 K compared to 293 K). The better overlap between the S_0 and S_1 potential energy curves and the decrease in energy between the two states should promote a better coupling between the radiationless modes of the excited- and ground-state thus enhancing the non-radiative decay channel with the concomitant decrease in ϕ_F at 77 K.

Fluorescence lifetimes (τ_F) collected in solution at 293 K did not reveal the presence of additional fast decay components that could be attributed to fast relaxation processes in the excited state (conformational relaxation or energy migration) thus in agreement with the existence of a rigid quinoidal-like structure in the excited state.

From the overall photophysical parameters (quantum yields and lifetimes) the rate constants for all the decay processes can be obtained. The radiative rate constants (k_F), for all the compounds (including **1a**) present a approximately constant value (0.315–0.363 ns^{-1}) thus showing that the decrease in ϕ_F for compound **1a** is not due to a decrease of this parameter but to an effective increase in the intersystem-crossing rate constant, k_{ISC} (1.17 ns^{-1} for **1a** *vs.* 0.055–0.089 ns^{-1} for **2a–c**).

Singlet oxygen was detected by its characteristic phosphorescence following triplet energy transfer from the compounds. The quantum yields for singlet oxygen formation are very close to the quantum yields for triplet formation thus providing support for the calculated latter values and showing that the sensitization of molecular singlet oxygen is very efficient ($S_\Delta = \phi_\Delta/\phi_T \approx 1$).

It is also worth noting that the different alkyl and aryl groups at position 1 of the pyrrole ring has no significant influence in the spectral and photophysical properties of the compounds (**2a**, **2b** and **2c**), see Tables 1 and 2.

Conclusions

We have investigated the spectroscopic and photophysical properties of thienylpyrrolyl-benzothiazole derivatives in solution at 293 and 77 K. It is shown that the position of the benzothiazole heterocycle on the thienylpyrrolyl system affects the extent of charge-transfer between the donor- and electron-acceptor groups and also induces profound changes in the photophysical properties. At room temperature, in general, placement of the benzothiazole group on the thienyl ring, when compared to the pyrrole ring, significantly enhances the radiative excited-state deactivation channel. This shows that the high fluorescence of the benzothiazole unit in conjugated organic oligomers and polymers can be tuned by the direct linking to the additional chromophoric unit, which in the present case was pyrrole *vs.* thiophene. In addition it was found that different groups (alkyl and aryl) at the nitrogen atom of the pyrrole ring have no effect on the spectral and photophysical properties of these compounds.

Acknowledgements

Thanks are due to the Foundation for Science and Technology (FCT-Portugal) for financial support through the Centro de Química-Universidade do Minho (Project PTDC/QUI/66251/2006). F. C. T. is acknowledged for a post-doctoral grant to J. Pina (SFRH/BPD/65507/2009) and a PhD grant to R. Batista (SFRH/BD/36396/2007). We also thank J. P. B. Santos and N. Gonçalves for some of the preliminary spectral measurements.

References

1 S. R. Marder, B. Kippelen, A. K. Y. Jen and N. Peyghambarian, *Nature*, 1997, **388**, 845–851.
2 Y. Q. Shi, C. Zhang, H. Zhang, J. H. Bechtel, L. R. Dalton, B. H. Robinson and W. H. Steier, *Science*, 2000, **288**, 119–122.
3 T. Baehr-Jones, M. Hochberg, G. X. Wang, R. Lawson, Y. Liao, P. A. Sullivan, L. Dalton, A. K. Y. Jen and A. Scherer, *Opt. Express*, 2005, **13**, 5216–5226.
4 A. Schneider and P. Gunter, *Ferroelectrics*, 2005, **318**, 83–88.
5 F. Kajzar, K. S. Lee and A. K. Y. Jen, in *Polymers for Photonics Applications II*, Springer, Berlin, 2003, vol. 161, pp. 1–85.
6 M. Q. He, T. M. Leslie, J. A. Sinicropi, S. M. Garner and L. D. Reed, *Chem. Mater.*, 2002, **14**, 4669–4675.
7 J. A. Davies, A. Elangovan, P. A. Sullivan, B. C. Olbricht, D. H. Bale, T. R. Ewy, C. M. Isborn, B. E. Eichinger, B. H. Robinson, P. J. Reid, X. Li and L. R. Dalton, *J. Am. Chem. Soc.*, 2008, **130**, 10565–10575.
8 L. R. Dalton, W. H. Steier, B. H. Robinson, C. Zhang, A. Ren, S. Garner, A. T. Chen, T. Londergan, L. Irwin, B. Carlson, L. Fifield, G. Phelan, C. Kincaid, J. Amend and A. Jen, *J. Mater. Chem.*, 1999, **9**, 1905–1920.
9 W. Wu, Z. Zhang and X. Zhang, *J. Chem. Res. (S)*, 2004, **2004**, 617–619.
10 A. K. Y. Jen, Y. Q. Liu, L. X. Zheng, S. Liu, K. J. Drost, Y. Zhang and L. R. Dalton, *Adv. Mater.*, 1999, **11**, 452–455.
11 P. Hrobarik, P. Zahradnik and W. M. F. Fabian, *Phys. Chem. Chem. Phys.*, 2004, **6**, 495–502.
12 J. M. Hao, M. J. Han, K. P. Guo, Y. X. Zhao, L. Qiu, Y. Q. Shen and X. G. Meng, *Mater. Lett.*, 2008, **62**, 973–976.

13 B. K. Spraul, S. Suresh, T. Sassa, M. A. Herranz, L. Echegoyen, T. Wada, D. Perahia and D. W. Smith, *Tetrahedron Lett*., 2004, **45**, 3253–3256.
14 K. P. Guo, J. M. Hao, T. Zhang, F. H. Zu, J. F. Zhai, L. Qiu, Z. Zhen, X. H. Liu and Y. Q. Shen, *Dyes Pigm*., 2008, **77**, 657–664.
15 P. Blanchard, J. M. Raimundo and J. Roncali, *Synth. Met*., 2001, **119**, 527–528.
16 Q. Q. Li, C. G. Lu, J. Zhu, E. Fu, C. Zhong, S. Y. Li, Y. P. Cui, J. G. Qin and Z. Li, *J. Phys. Chem. B*, 2008, **112**, 4545–4551.
17 Z. A. Li, Z. Li, C. A. Di, Z. C. Zhu, Q. Q. Li, Q. Zeng, K. Zhang, Y. Q. Liu, C. Ye and J. G. Qin, *Macromolecules*, 2006, **39**, 6951–6961.
18 Z. A. Li, Q. Zeng, Z. Li, S. C. Dong, Z. C. Zhu, Q. Q. Li, C. Ye, C. A. Di, Y. Q. Liu and J. G. Qin, *Macromolecules*, 2006, **39**, 8544–8546.
19 P. R. Varanasi, A. K. Y. Jen, J. Chandrasekhar, I. N. N. Namboothiri and A. Rathna, *J. Am. Chem. Soc*., 1996, **118**, 12443–12448.
20 M. M. M. Raposo, A. Sousa, G. Kirsch, P. Cardoso, M. Belsley, E. D. Gomes and A. M. C. Fonseca, *Org. Lett*., 2006, **8**, 3681–3684.
21 R. M. F. Batista, S. P. G. Costa, E. L. Malheiro, M. Belsley and M. M. M. Raposo, *Tetrahedron*, 2007, **63**, 4258–4265.
22 R. M. F. Batista, S. P. G. Costa, M. Belsley and M. M. M. Raposo, *Tetrahedron*, 2007, **63**, 9842–9849.
23 R. M. F. Batista, S. P. G. Costa and M. M. M. Raposo, *Tetrahedron Lett*., 2004, **45**, 2825–2828.
24 S. P. G. Costa, R. M. F. Batista, P. Cardoso, M. Belsley and M. M. M. Raposo, *Eur. J. Org. Chem*., 2006, 3938–3946.
25 R. S. Becker, J. Seixas de Melo, A. L. Maçanita and F. Elisei, *J. Phys. Chem*., 1996, **100**, 18683–18695.
26 M. Montalti, A. Credi, L. Prodi and M. T. Gandolfi, *Handbook of Photochemistry*, CRC Press, Boca Raton, FL, 2006.
27 J. Pina, J. Seixas de Melo, H. D. Burrows, A. L. Maçanita, F. Galbrecht, T. Bunnagel and U. Scherf, *Macromolecules*, 2009, **42**, 1710–1719.
28 G. Striker, V. Subramaniam, C. A. M. Seidel and A. Volkmer, *J. Phys. Chem. B*, 1999, **103**, 8612.
29 J. Pina, H. D. Burrows, R. S. Becker, F. B. Dias, A. L. Maçanita and J. Seixas de Melo, *J. Phys. Chem. B*, 2006, **110**, 6499–6505.
30 J. Pina, J. Seixas de Melo, H. D. Burrows, A. Bilge, T. Farrell, M. Forster and U. Scherf, *J. Phys. Chem. B*, 2006, **110**, 15100–15106.
31 R. V. Bensasson, E. J. Land and T. G. Truscott, *Excited States and Free Radicals in Biology and Medicine*, Oxford Science Publications, Oxford, 1993.
32 C. V. Kumar, L. Qin and P. K. Das, *J. Chem. Soc., Faraday Trans. 2*, 1984, **80**, 783–793.
33 C. Flors and S. Nonell, *Helv. Chim. Acta*, 2001, **84**, 2533–2539.
34 M. J. Frisch, G. W. Trucks, H. B. Schlegel, G. E. Scuseria, M. A. Robb, J. R. Cheeseman, J. A. Montgomery, Jr., T. Vreven, K. N. Kudin, J. C. Burant, J. M. Millam, S. S. Iyengar, J. Tomasi, V. Barone, B. Mennucci, M. Cossi, G. Scalmani, N. Rega, G. A. Petersson, H. Nakatsuji, M. Hada, M. Ehara, K. Toyota, R. Fukuda, J. Hasegawa, M. Ishida, T. Nakajima, Y. Honda, O. Kitao, H. Nakai, M. Klene, X. Li, J. E. Knox, H. P. Hratchian, J. B. Cross, V. Bakken, C. Adamo, J. Jaramillo, R. Gomperts, R. E. Stratmann, O. Yazyev, A. J. Austin, R. Cammi, C. Pomelli, J. Ochterski, P. Y. Ayala, K. Morokuma, G. A. Voth, P. Salvador, J. J. Dannenberg, V. G. Zakrzewski, S. Dapprich, A. D. Daniels, M. C. Strain, O. Farkas, D. K. Malick, A. D. Rabuck, K. Raghavachari, J. B. Foresman, J. V. Ortiz, Q. Cui, A. G. Baboul, S. Clifford, J. Cioslowski, B. B. Stefanov, G. Liu, A. Liashenko, P. Piskorz, I. Komaromi, R. L. Martin, D. J. Fox, T. Keith, M. A. Al-Laham, C. Y. Peng, A. Nanayakkara, M. Challacombe, P. M. W. Gill, B. G. Johnson, W. Chen, M. W. Wong, C. Gonzalez and J. A. Pople, *GAUSSIAN 03 (Revision C.02)*, Gaussian, Inc., Wallingford, CT, 2004.
35 A. D. Becke, *J. Chem. Phys*., 1993, **98**, 1372–1377.
36 M. M. Francl, W. J. Pietro, W. J. Hehre, J. S. Binkley, M. S. Gordon, D. J. Defrees and J. A. Pople, *J. Chem. Phys*., 1982, **77**, 3654–3665.
37 J. B. Foresman, M. Headgordon, J. A. Pople and M. J. Frisch, *J. Phys. Chem*., 1992, **96**, 135–149.
38 S. Portmann and H. P. Luthi, *Chimia*, 2000, **54**, 766–770.
39 J. Pina, J. Seixas de Melo, H. D. Burrows, R. M. F. Batista, S. P. G. Costa and M. M. M. Raposo, *J. Phys. Chem. A*, 2007, **111**, 8574–8578.
40 S. Rentsch, J. P. Yang, W. Paa, E. Birckner, J. Schiedt and R. Weinkauf, *Phys. Chem. Chem. Phys*., 1999, **1**, 1707–1714.
41 D. Wasserberg, P. Marsal, S. C. J. Meskers, R. A. J. Janssen and D. Beljonne, *J. Phys. Chem. B*, 2005, **109**, 4410–4415.
42 J. Seixas de Melo, F. Elisei and R. S. Becker, *J. Chem. Phys*., 2002, **117**, 4428–4435.
43 J. Pina, J. Seixas de Melo, R. Batista, S. Costa and M. M. Raposo, *J. Phys. Chem. B*, 2010, **114**, 4964–4972.
44 D. S. Zyss, *Non-linear Optical Properties of Organic Molecules and Crystals*, Academic Press, Orlando, FL, 1987.
45 R. D. Miller, V. Y. Lee and C. R. Moylan, *Chem. Mater*., 1994, **6**, 1023–1032.